INTERNATIONAL JOURNAL OF PRECISION ENGINEERING AND MANUFACTURING Vol. 15, No. 3, pp. 447-454 MARCH 2014 / 447
DOI: 10.1007/s12541-014-0356-3

# Optimization of Hybrid $CO_2$ Laser-GMA Welding Parameters on Dissimilar Materials AH32/STS304L using Grey-based Taguchi Analysis

**Sung-Min Joo[1], Han-Sur Bang[2,#], and Si-Young Kwak[3]**

1 Plant R &D Division, Research Institute of Industrial Science &Technology, Ulsan 683-420, Korea
2 Department of Naval Architecture and Ocean Engineering, Chosun University, Gwangju 501-759, Korea
3 E-Design Center, Korea Institue of Industrial Technology (KITECH), Incheon 406-840, Korea
# Corresponding author / E-mail: hsbang@chosun.ac.kr, TEL: +82-62-230-7134, FAX: +82-62-223-5648

KEYWORDS: Hybrid $CO_2$ laser-GMA welding, Dissimilar materials, Grey-based taguchi analysisd

*This study intended to verify the feasibility of laser-arc hybrid welding to dissimilar materials joints between high strength steel (AH32) and stainless steel (STS304L). For this, hybrid welding process for dissimilar materials was optimized by varying four parameters (welding speed, welding current, laser-arc distance, welding voltage) through Grey-based Taguchi analysis. A Grey relational analysis of the ultimate tensile strength (UTS), welding depth to width ratio (D/W) and absorbed energy (AE) attained from the Taguchi method can optimize the multiple-performance characteristics of the Grey relational grade. Moreover, hardness values microstructure and fatigue strength of welded joints fabricated under welding condition optimized by Grey-based Taguchi analysis were investigated. In the tensile test of welded joints, the damaged part was in BM of STS304L side. The hardness of welded joints exhibits within the acceptable range (the maximum value 340~360 Hv). Dissimilar materials hybrid welded joints exhibited almost same fatigue strength for similar material STS304L SAW welded joints and lied well above the design curve(level D) for JSSC.*

Manuscript received: June 10, 2013 / Revised: December 10, 2013 / Accepted: January 12, 2014

## 1. Introduction

Steel structures can be made more functionally and economically with the fabrication of structural members using dissimilar materials. It is often desired to use dissimilar materials (high strength steel and stainless steel) to provide higher strength and performance to bridges, ships, offshore structures, and pipelines. Laser-arc hybrid welding has been in spotlight recently as a revolutionary method in manufacturing industries due to its high welding speed, low distortion, deep penetration, high mechanical properties.[1-4] And the process is much more tolerant to joint fit-up variations than laser welding, maintaining its deep penetration. This enables the full penetration welds of thick plates, which eliminates multiple passes and reduces after welding work such as cutting for adjustment and fairing at the assemble stage. The application of laser-arc hybrid welding to dissimilar materials between high strength steels and stainless steels offers substantial advantages to large structures[8,9] because it secures safety against catastrophes due to weld defects.

In the laser-arc hybrid welding, the combination of two different heat sources provides several merits, however, it also determines several technological problems. Some of these problems concern the stability of the process, mainly related to the shielding gas composition,[15,16] droplet transfer mode,[17,18] arc current[19,20] sources position and mutual interaction.[21-23] Most studies have addressed the effect of the fundamental process parameters for hybrid welding. In particular, the combination of these parameters creates a complicated reaction during welding process.

Therefore, this study intend to optimize laser-arc hybrid welding parameters with multiple performance characteristics to dissimilar materials joints between high strength steel (AH32) and stainless steel (STS304L).

For this, hybrid welding process in dissimilar materials was optimized via Grey-based Taguchi analysis[9,10] that has a broad field of application in manufacturing processes, which solve multi-objective optimization problem simultaneously. Moreover, the analysis of variance (ANOVA) and confirmation test were conducted to clarify the experimental results

## 2. Research Method

### 2.1 Experimental details

AH32 and STS304L plates (600 mm (L) × 250 mm (B) × 13 mm (t)) were used for butt welding of dissimilar materials (AH32-STS304L) at zero gap conditions. Continuous wave $CO_2$ laser with a maximum output power of 12 kw was used as the laser power source. Inverter welder with a rated output of 500 A was used as the GMA power source and push-pull GMAW torch was utilized for feeding of the welding wire. Shielding gas was supplied through a GMAW torch located at the side of laser head. The arc leading laser-arc hybrid welding was implemented, where the laser beam was focused perpendicular on the surface of the specimen. Laser focal distance of 250 mm which allowed a minimum spot diameter of 0.8 mm and contact tip to work distance (CTWD) of 20 mm were kept constant throughout the welding process. The laser beam focal position was constantly kept on the upper surface of the work-piece. The angle between the electrode and the welding direction is 45°. GMAW wire (AWS A5.9 ER309L, 1.2 mm diameter) was used in the experiments for dissimilar materials welding. The hybrid welding process for dissimilar materials was optimized by varying process parameters through Grey-based Taguchi analysis. The hybrid welding process for dissimilar materials was optimized by varying four parameters (welding speed, welding current, laser-arc distance, welding voltage) in this study. Welding experiment is repeated three times under same condition.

Hybrid welding condition for dissimilar materials was made allowance for the hybrid welding conditions obtained from the butt welding of similar materials (AH32-AH32, STS304L-STS304L) that were determined through mechanical and metallurgical characteristics evaluation as well as welding phenomena observation with high speed video camera by varying selected four parameters (shielding gas composition ratio, welding speed, laser power, laser-arc distance) in previous study.[11]

In the experiments, shielding gas compositions of He65%, Ar32%, $CO_2$ 3% for spray transfer mode, was adopted during hybrid welding, which produced consistent bead width and appearance with a stable arc formation and little spatter generation.

In this study, the reinforcement, back-bead, undercut and uniformity of weld bead were considered as the evaluation indices for welds and the welding conditions were determined by evaluating the effect of welding process variables based on the welding defect standard (EN ISO 13919-1) for electron beam and laser welding.[12] Hardness measurement and fatigue tests[12-14] of welded joints fabricated under welding condition optimized by Grey-based Taguchi analysis in section 3.2.(A) were carried out.

Hardness values at distances of 3 mm and 12 mm over the bottom surface of welded joints were carried out.

The fatigue tests for dissimilar materials AH32-STS304L hybrid welded joints were carried out under pulsating tensile loading with the stress ratio R = ($P_{min}/P_{max}$) = 0.1. The fatigue test specimen was selected in the transverse direction of welded specimen as shown in Fig. 2(a). The dimensions of specimen were chosen according to the standard ASTM E466.

The dimensions of the fatigue specimen are length of 140.5 mm, width of 15 mm and thickness of 3.0 mm. as shown in Fig. 2(b). The

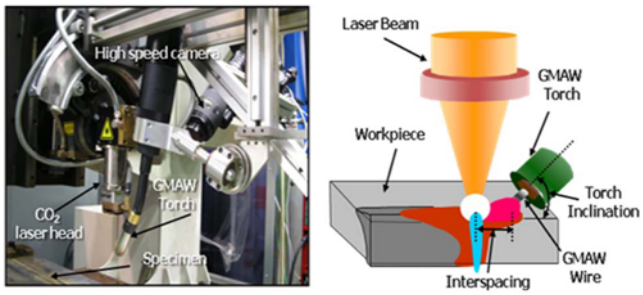


Fig. 1 Experimental set-up for hybrid welding

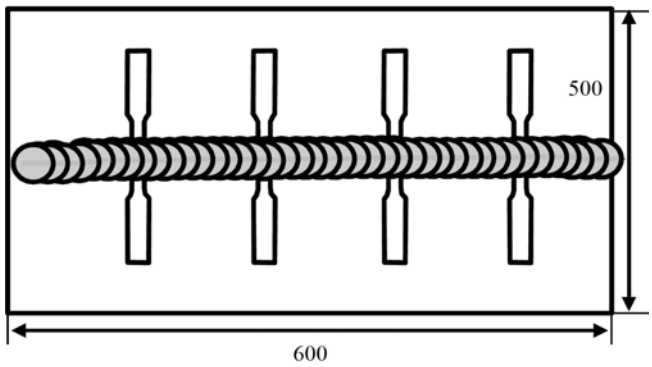


(a) Scheme of extraction from the welded plates

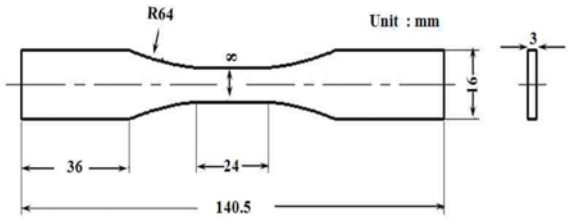


(b) Geometry of the fatigue test specimen

Fig. 2 Dimension of the fatigue test specimen

applied cyclic loading waveform was sinusoidal and the frequency of loading used was varied from 55 to 57 Hz according to the load amplitude.

### 2.2 Optimization of welding process via Grey-based Taguchi analysis

#### 2.2.1 Experimental procedure

Optimum welding process parameters, which considered the multiple performance characteristics, were acquired. The initial values of the welding parameters were welding speed of 1.3 m/min, arc current of 300 A, laser-arc distance of 0 mm, and arc voltage of 28 V. Welding experiments for determining the optimal welding parameters were carried out by setting the welding speed at 1.3 or 1.5 m/min, arc current at 260 or 280 or 300 A, laser-arc distance at 0 or 2 or 4 mm and arc voltage at 23 or 25 or 28 V.

The summary of experimental conditions is shown in Table 3. The experimental results after hybrid welding were estimated in terms of the following measured performance: (1) ultimate tensile strength (UTS), (2) welding depth to width ratio (D/W) and (3) absorbed energy (AE)

Table 1 Hybrid welding parameters and their levels (* Initial process parameters)

| Factors | Parameter | Level1 | Level 2 | Level 3 |
|---|---|---|---|---|
| A | Welding speed (m/min) | 1.3* | 1.5 | - |
| B | Welding current (A) | 230 | 280 | 300* |
| C | Laser-arc distance (mm) | 0 | 2 | 4* |
| D | Welding voltage (V) | 23* | 25 | 27 |

of charpy impact test results of welded specimen. In order to attain supreme weldability, Taguchi's experimental design was utilized for conducting experiments. For this, a $L_{18}$ orthogonal array was used for the experiment.

### 2.2.2 Determination of welding process parameters

The welding parameters were determined by the Grey-based Taguchi method.

#### 2.2.2.1 Orthogonal arrays

Taguchi's method determined the domineering factors incorporated in the optimization for hybrid welding. In this welding process, the four welding parameters such as welding speed, welding current, laser-arc distance and welding voltage were considered, at two or three different levels respectively. Among these four parameters, welding speed at two-levels were considered and the others (welding current, laser-arc distance and welding voltage) were considered at three-levels.

Therefore, a total of 54(2x3x3x3) different combinations were considered. According to Taguchi, however, the samples could be classified into 18 groups.

Table 2 illustrates the grouping of the samples into 18 groups according to Taguchi. The numbers indicate the various experimental arrangements or levels of the differing factors.

In Table 3, the experimental results were summarized.

#### 2.2.2.2 Grey relational analysis

Grey analysis was used in evaluating the performance of a complicated design. Nevertheless, the data applied in Grey analysis was demanded to be pre-processed into quantitative indices to normalize raw data for analysis.

*1) Data pre-processing*

Data pre-processing is a process of assigning the original sequence to a comparable sequence. For this, the experimental raw results are normalized in the range between zero and one.

The three necessities such as ultimate tensile strength, welding depth to width ratio and absorbed energy in welded joints in this study correlate with the definition of "the-higher-the-better type. When the form "the-higher-the-better becomes the anticipated value of the data sequence, the original sequence is normalized as follows.

$$x_i^*(k) = \frac{x_i^o(k) - \min x_i^o(k)}{\max x_i^o(k) - \min x_i^o(k)} \quad (1)$$

Where, $x_i^o(k)$ is the original sequence, $x_i^*(k)$ is a normalized value of kth element in the ith sequence, $\max x_i^o(k)$ is the largest value of $x_i^o(k)$, and $\min x_i^o(k)$ is the smallest value of $x_i^o(k)$.

However, if there is "a specific desired value", then original sequence can be normalized using this equation.

Table 2 Experiment layout using $L_{18}$ orthogonal arrays

| Group no. | Factor A | Factor B | Factor C | Factor D |
|---|---|---|---|---|
| 1 | 1 | 1 | 1 | 1 |
| 2 | 1 | 1 | 2 | 2 |
| 3 | 1 | 1 | 3 | 3 |
| 4 | 1 | 2 | 1 | 1 |
| 5 | 1 | 2 | 2 | 2 |
| 6 | 1 | 2 | 3 | 3 |
| 7 | 1 | 3 | 1 | 2 |
| 8 | 1 | 3 | 2 | 3 |
| 9 | 1 | 3 | 3 | 1 |
| 10 | 2 | 1 | 1 | 3 |
| 11 | 2 | 1 | 2 | 1 |
| 12 | 2 | 1 | 3 | 2 |
| 13 | 2 | 2 | 1 | 2 |
| 14 | 2 | 2 | 2 | 3 |
| 15 | 2 | 2 | 3 | 1 |
| 16 | 2 | 3 | 1 | 3 |
| 17 | 2 | 3 | 2 | 1 |
| 18 | 2 | 3 | 3 | 2 |

Table 3 Average ultimate tensile strength, welding depth and width ratio and absorbed energy

| Group no. | Ultimate tensile strength (MPa) | Depth and width ratio | Absorbed energy (J) |
|---|---|---|---|
| 1 | 444 | 1.927 | 128 |
| 2 | 462 | 1.93 | 133 |
| 3 | 476 | 1.931 | 140 |
| 4 | 483 | 1.933 | 142 |
| 5 | 489 | 1.943 | 154 |
| 6 | 492 | 1.95 | 166 |
| 7 | 494 | 1.958 | 188 |
| 8 | 501 | 1.959 | 206 |
| 9 | 508 | 1.959 | 207 |
| 10 | 424 | 1.799 | 82 |
| 11 | 442 | 1.891 | 87 |
| 12 | 456 | 1.906 | 94 |
| 13 | 463 | 1.914 | 98 |
| 14 | 468 | 1.917 | 102 |
| 15 | 470 | 1.929 | 106 |
| 16 | 474 | 1.931 | 118 |
| 17 | 480 | 1.932 | 122 |
| 18 | 488 | 1.938 | 130 |

$$x_i^*(k) = 1 - \frac{\left| x_i^o(k) - x^o \right|}{\max\{\max x_i^o(k) - x^o; x^o - \min x_i^o(k)\}} \quad (2)$$

Where, $x^o$ is the desired value of the kth quality characteristics.

*2) Grey relational coefficient and Grey relational grade*

After data pre-processing is carried out, a grey relational coefficient can be computed to specify relation between the ideal and actual normalized experiment results. The grey relational coefficient can be defined as follows.[6]

$$\xi_i(k) = \frac{\Delta_{min} + \xi \cdot \Delta_{max}}{\Delta_{0i}(k) + \xi \cdot \Delta_{max}} \quad (3)$$

Where, $\Delta_{0i}(k)$ is the absolute value of difference between the reference sequence $x_0^*(k)$ and the comparability sequence $x_i^*(k)$.

$$\Delta_{0i}(k) = \left| x_o^*(k) - x_i^*(k) \right| \tag{4}$$

$$\Delta_{max} = \max_{\forall j \in i} \max_{\forall k} \left| x_0^*(k) - x_j^*(k) \right| \tag{5}$$

$$\Delta_{min} = \min_{\forall j \in i} \min_{\forall k} \left| x_0^*(k) - x_j^*(k) \right| \tag{6}$$

$\xi$ is identifying coefficient and $\xi = 0.5$ is generally used.

Generally, the average of the grey relational coefficient is taken as the grey relational grade after attaining the grey relational coefficient. The grey relational grade is represented as follows:

$$\Gamma_i = \frac{1}{n} \sum_{k=1}^{n} \xi_i(k) \tag{7}$$

The grade $\Gamma_i$ suggests the correspondence between the reference sequence and the specific sequence $x_i$. Since the grade, $\Gamma_i$ has been evaluated through considering three requirements, the highest grade among all 18 groups precisely signifies the optimized combination for hybrid welding.

## 3. Analysis and Discussion

### 3.1 Experimental results

In this study, UTS (ultimate tensile strength), D/W (welding depth to width ratio) and AE (absorbed energy) under different welding parameters and experiments are shown in Tables 4.

The data sequences had a the-higher-the-better characteristic. The values of UTS, D/W and AE were applied to the reference sequence $x_0^*$ ($k$ = 1~3) The results of 18 experiments were the comparability sequence $x_i^*$ ($k$, $i$ = 1, 2, …, 18, $k$ = 1~3).

Table 4 shows all sequences, which following data pre-processing using Eq. (1). Moreover, the deviation sequences $\Delta_{0i}(k)$, $\Delta_{max}(k)$ and $\Delta_{min}(k)$ for $i$ = 1~18, $k$ = 1~3 can be computed in Eq. (4)~(6). Table 5 lists the Grey relational coefficient and grade for each case of the $L_{18}$ orthogonal array by using Eq. (3) and (7). According to the designed layout of the experiment, it was obtained from Table 5 that the setting of the hybrid welding parameters values in experiment No.9 had the highest Grey relation grade, which offered the best multi-performance characteristics out of the 18 experiments.

In order to calculate the average grey relational grade for each factor level, the response of the Taguchi method was applied. The process categorized the relational grade primarily by the factor level for each column in the orthogonal array, and then averages them. Hence, the comparability sequence had a larger value of Grey relational grade for the UTS, D/W and AE. Derived from this assumption, this study selected the level that supplied the largest average response.

In Table 6, A1, B3, C3 and D3 illustrate the largest value of Grey relational grade for factors A, B, C and D respectively, which suggest the optimal parameter combination of the hybrid welding process.

The Grey relational grade graph in Fig. 3 demonstrated the change in the response, when the factors are varied for their level 1- level 2 or level 3. This figure, the greater values gave the high UTS, D/W and AE. When the last column of Table 6 was compared, it was observed that the difference between the maximum and the minimum value of the Grey relational grade for factor B was the greatest. This suggests that the welding current has a stronger influence on the multi-performance characteristics.

Table 4 Sequence of each performance characteristic after data preprocessing

| Group no. | UTS (MPa) | D/W | AE (J) |
|---|---|---|---|
| Reference sequence | 1 | 1 | 1 |
| 1 | 0.232558 | 0.7911 | 0.359375 |
| 2 | 0.44186 | 0.809642 | 0.398438 |
| 3 | 0.604651 | 0.815822 | 0.453125 |
| 4 | 0.686047 | 0.828183 | 0.46875 |
| 5 | 0.755814 | 0.889988 | 0.5625 |
| 6 | 0.790698 | 0.933251 | 0.65625 |
| 7 | 0.813953 | 0.952695 | 0.828125 |
| 8 | 0.895349 | 0.988875 | 0.96875 |
| 9 | 0.976744 | 0.988875 | 0.976563 |
| 10 | 0 | 0 | 0 |
| 11 | 0.209302 | 0.568603 | 0.039063 |
| 12 | 0.372093 | 0.66131 | 0.09375 |
| 13 | 0.453488 | 0.710754 | 0.125 |
| 14 | 0.511628 | 0.729295 | 0.15625 |
| 15 | 0.534884 | 0.803461 | 0.1875 |
| 16 | 0.581395 | 0.815822 | 0.28125 |
| 17 | 0.651163 | 0.822002 | 0.3125 |
| 18 | 0.744186 | 0.859085 | 0.375 |

Table 5 Grey relational coefficients and grades for 18 groups

| Group | Grey relational coefficient | | | Grey relational grade | |
|---|---|---|---|---|---|
| no. | UTS | D/W | AE | $\gamma_i$ | Rank |
| 1 | 0.3945 | 0.70532 | 0.43836 | 0.512723 | 13 |
| 2 | 0.47253 | 0.72426 | 0.4539 | 0.55023 | 11 |
| 3 | 0.55844 | 0.7308 | 0.47761 | 0.588952 | 8 |
| 4 | 0.61429 | 0.74425 | 0.48485 | 0.614461 | 7 |
| 5 | 0.67188 | 0.81966 | 0.53333 | 0.674955 | 5 |
| 6 | 0.70492 | 0.88222 | 0.59259 | 0.726578 | 4 |
| 7 | 0.72881 | 0.96655 | 0.74419 | 0.813182 | 3 |
| 8 | 0.82692 | 0.97823 | 0.94118 | 0.915445 | 2 |
| 9 | 0.95556 | 0.97823 | 0.95522 | 0.963005 | 1 |
| 10 | 0.33333 | 0.33333 | 0.33333 | 0.333333 | 18 |
| 11 | 0.38739 | 0.53683 | 0.34225 | 0.422154 | 17 |
| 12 | 0.4433 | 0.59617 | 0.35556 | 0.465008 | 16 |
| 13 | 0.47778 | 0.63352 | 0.36364 | 0.491643 | 15 |
| 14 | 0.50588 | 0.64876 | 0.37209 | 0.508911 | 14 |
| 15 | 0.51807 | 0.71783 | 0.38095 | 0.538953 | 12 |
| 16 | 0.5443 | 0.7308 | 0.41026 | 0.561788 | 10 |
| 17 | 0.58904 | 0.73747 | 0.42105 | 0.58252 | 9 |
| 18 | 0.66154 | 0.78014 | 0.44444 | 0.628706 | 6 |

Table 6 Response for the grey relational grade (*Optimal level)

| Welding parameters | Level 1 | Level 2 | Level 3 | Max-Min |
|---|---|---|---|---|
| A | 0.706615* | 0.503668 | | 0.202946 |
| B | 0.478733 | 0.592584 | 0.744108* | 0.265374 |
| C | 0.554522 | 0.609036 | 0.651867* | 0.097345 |
| D | 0.605636 | 0.603954 | 0.605835* | 0.001881 |

### 3.2 Confirmation test

The final step is to validate the improvement of the performance

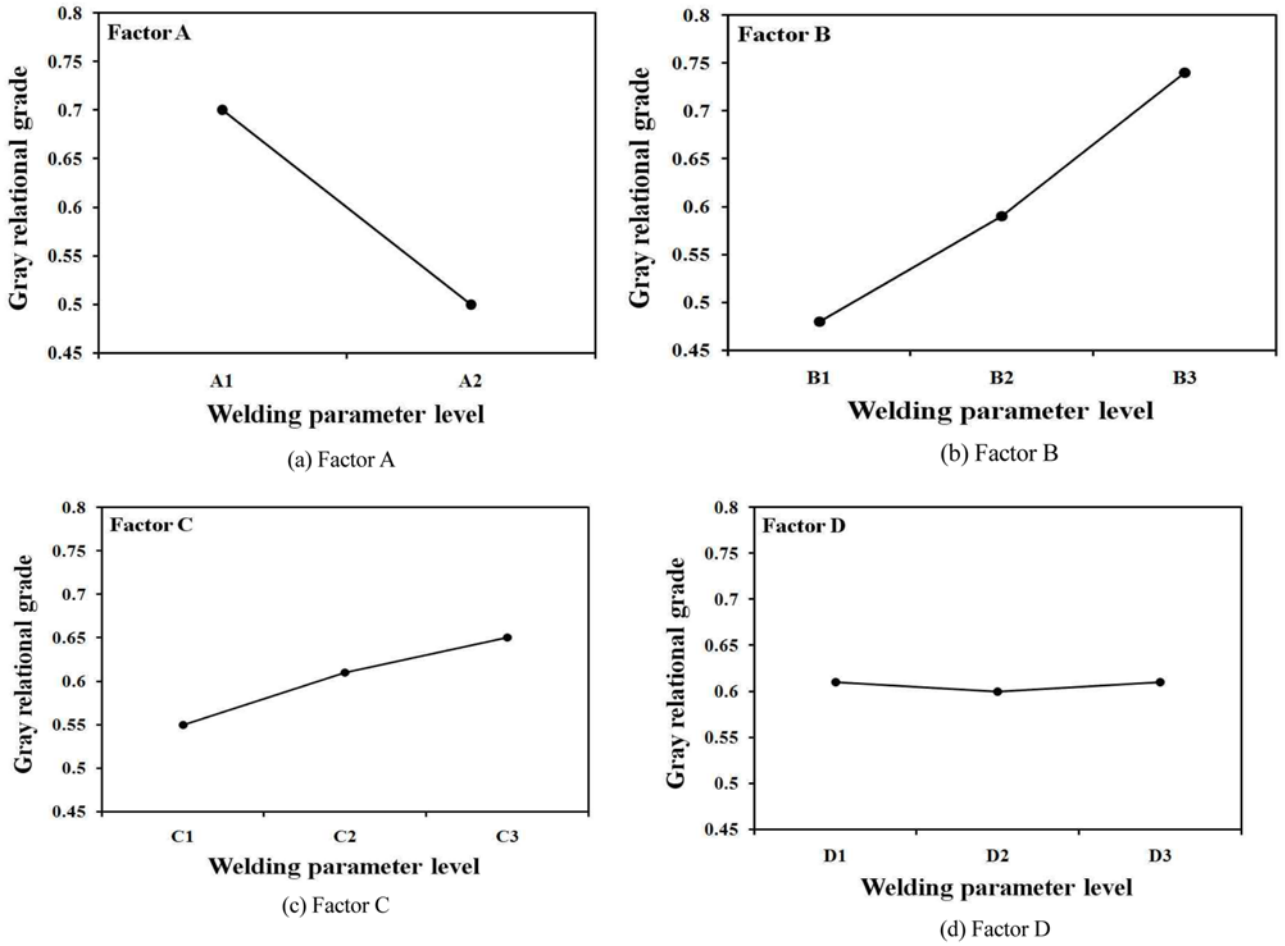


Fig. 3 Graph of grey relational grade

Table 7 Results of welding performance using the initial and optimal welding process parameters

| | Initial process parameters | Optimal process parameters |
|---|---|---|
| Level | A1B3C3D1 | A1B3C3D3 |
| UTS | 502 | 508 |
| D/W | 1.948 | 1.959 |
| AE | 202 | 207 |

characteristics by using the optimum levels of the welding process parameters.

Table 7 shows the comparison of experimental results attained using the initial and optimal welding process parameters. As shown in Table 7, UTS was increased from 502 to 508, D/W was increased from 1.948 to 1.959, and AE was increased from 202 to 207.

### 3.3 Development of welding process

#### 3.3.1 Grey relational analysis

A Grey relational analysis of the UTS, D/W and AE attained from the Taguchi method can optimize the multiple-performance characteristics of the Grey relational grade. Conclusively, it was found that the performance characteristics of the hybrid welding process such as UTS, D/W and AE are enhanced. Details on welding condition are given in Table 8. Cross section of butt welded joints is shown in Fig. 4. Fig. 5 shows high speed photographs of droplet transfer (spray mode) for He65% + Ar32% + $CO_2$3% shielding gas in hybrid welding with optimized parameters.

Table 8 Hybrid welding condition for dissimilar materials AH32-STS 304L

| Item | | Paeametersa |
|---|---|---|
| $CO_2$ Laser power (kW) | | 12 |
| GMAW | Wire type | AWS A5.9 ER309L |
| | Voltage (V) | 27 |
| | Current (A) | 300 |
| | CTWD (mm) | 20 |
| | Wire feeding speed (mm/min) | 9.8 |
| Welding speed( mm/min) | | 1,300 |
| Interspacing (mm) | | 4 |
| Gap (mm) | | 0 |
| Shielding gas | | He65%, Ar32%, $CO_2$ 3% |

The bead width and reinforcement are 9 mm and 2 mm, respectively, and the bead width of AH32 side was about 1 mm greater than that of STS304L mainly due to the thermal conductivity difference between the two base metals, that is, the thermal conductivity of AH32 is higher than that of STS304L. Back bead width and height were 1 mm and 0.3 mm, respectively, and the welded joints showed a well balanced bead cross section with sufficient reinforcement and controlled excessive back bead.

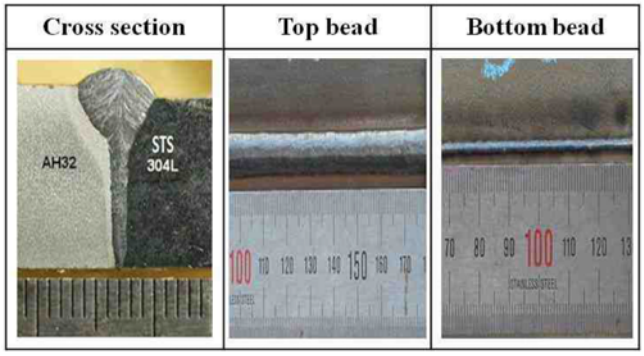


Fig. 4 Bead surface appearance and cross section of AH32-STS304L hybrid butt welded joints

Fig. 5 High speed photographs of droplet transfer for He65% + Ar32% + $CO_2$3% shielding gas in hybrid welding with optimized parameters

Moreover, defects such as undercut and porosity was not formed in the microstructure; therefore, the initial visual test of the welds could be classified as very stringent (Quality B') in quality levels for weld imperfections based on EN ISO 13919-1.

### 3.3.2 Hardness and Microstructure

Hardness measurement of welded joints fabricated under welding condition optimized by Grey-based Taguchi analysis in section 3.2.(A) was carried out. Measured values at distances of 3 mm and 12 mm over the bottom surface of welded joints are shown in Fig. 6.

From the result shown in Fig. 6, it was found that the hardness values at distances of 3 mm and 12 mm over the bottom surface of hybrid welds were in the order of WM > HAZ > BM.

The hardness at distance of 3 mm over the bottom surface was higher than that at distance of 12 mm over bottom surface, whose lower part was affected mainly by rapid heating and cooling characteristics of laser process.

In addition, the hardness of WM in AH32 was higher than that of STS304L due to the much more rapid heating and cooling rate. Difference between the hardness value in HAZ and that in BM is not so large at y = 12 mm; however, at y = 3 mm, away from the bottom surface, the hardness in HAZ was significantly higher than that of BM.

Comparing the hardness value of WM and BM at distance of 3 mm

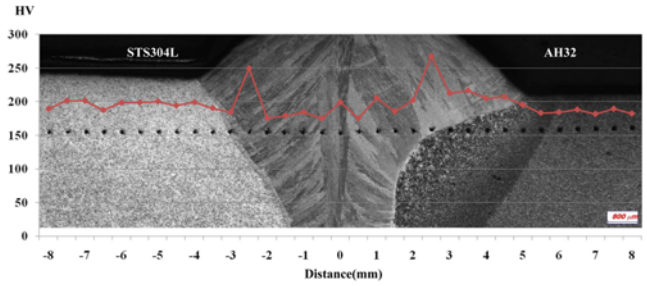


(a) 12 mm over bottom surface

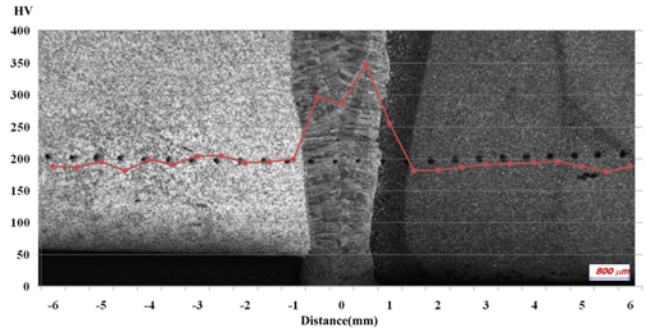


(b) 1 mm over bottom surface

Fig. 6 Distribution of hardness in dissimilar materials hybrid welded joints

over the bottom surface, general hardness values of STS304L and AH32 used in experiment were approximately 195 Hv and 182 Hv; however, the maximum hardness values of WM were 297 Hv and 348 Hv.

Fig. 7 shows the microstructures microstructural in Weld metal (WM), Heat affected zone (HAZ) and Base metal (BM) regions of dissimilar materials hybrid welded joints.

The microstructures of the WM exhibits well distributed plate-like shaped ferrite in the matrix instead of a dendritic structure. Well developed dendritic structure is formed in HAZ. The HAZ size at the AH32 side of the welds is about 120~150 $\mu$m, and the HAZ size at the STS304L side of the welds is about 60~100 $\mu$m.

The microstructure of the base metal AH32 exhibits a coexisting structure of both ferrite (bright contrast) and pearlite (black band). The microstructure of the base metal STS304L shows an austenitic structure with grain size of about 10~60 $\mu$m.

### 3.3.3 Fatigue strength

Fatigue strength of welded joints fabricated under welding condition optimized by Grey-based Taguchi analysis in section 3.2.(A) were investigated. The fatigue strength is determined in the life range $10^4$~$10^7$ cycles. Fatigue life is defined as the cycle number during which a specimen is divided into two parts, and the fatigue limit is considered to be $10^7$ cycles.

Fig. 8 represents the S-N diagrams of the dissimilar materials hybrid welded joints compared with that of similar material STS304L SAW welded joints and design curve of JSSC.

Fatigue fracture occurred at STS304L side of BM in dissimilar materials hybrid welded joints. It can be inferred that because the specific strength of STS 304L is smaller than that of AH32, where STS 304L has approximately less than half yield stress and tensile strength than that of AH32.

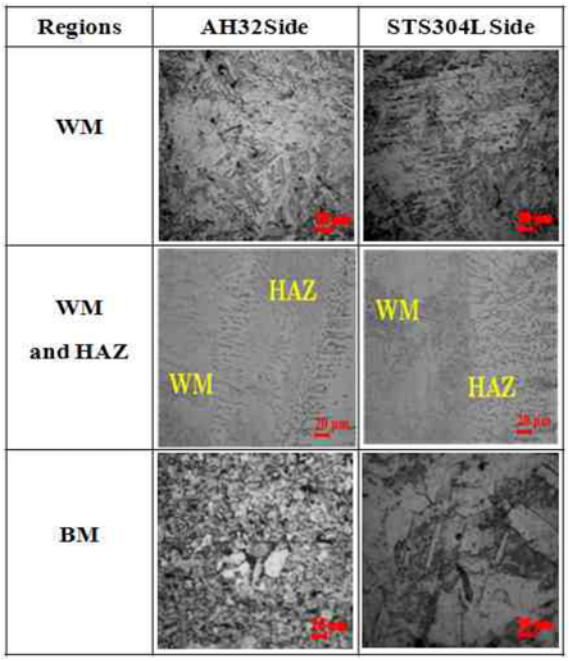


Fig. 7 Microstructural in WM, HAZ and BM regions of dissimilar materials hybrid welded joints

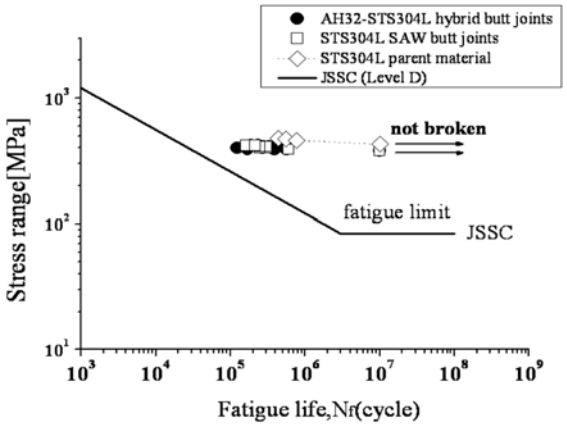


Fig. 8 S-N diagrams of the dissimilar materials hybrid welded joints

From the figure, the fatigue curve obtained lied well above the design curve for JSSC. Dissimilar materials hybrid welded joints exhibited nearly the same as fatigue strength and limit of similar material STS 304L SAW welded joints, however, exhibited lower fatigue limit than BM of STS304L. It was noteworthy that the welded joints of dissimilar materials exhibited similar fatigue strength to the STS304L SAW welded joints and lied well above the design curve (level D) for JSSC.

## 4. Conclusions

1. The optimum conditions for hybrid butt welded joints of 13 mm AH32 and STS304L steel plate was current of 300 A, voltage of 27 V, welding speed of 1.3 m/min, shielding gases 65%He + 32%Ar + 3% $CO_2$, CTWD of 20 mm, the spacing between the laser spot and the filler wire tip of 4 mm and laser power of 12 kW.

2. It was found that the initial visual test of the welds can be classified as very stringent (Quality B') in quality levels for weld imperfections such as reinforcement, back-bead, undercut and uniformity of weld bead based on EN ISO 13919-1.

3. Tensile strength of hybrid welded joints was about 502 MPa. In the tensile test of welded joints, the damaged part was in BM of STS 304L side. Tensile strength of welded joints in dissimilar materials was comparable to that of STS304L base material.

4. Hardness values at distances of 3 mm and 12 mm over the bottom surface of welds were in the order of WM > HAZ > BM. The hardness at distance of 3 mm over the bottom surface was higher than that at distance of 12 mm over the bottom surface. The hardness of WM in AH32 was higher than that of STS304L due to its much more rapid heating and cooling rate. The hardness of hybrid welded joints exhibited within the acceptable range (the maximum value 340~360 Hv).

5. Dissimilar materials hybrid welded joints exhibited almost same fatigue strength for similar material STS304L SAW welded joints and lied well above the design curve (level D) for JSSC. This indicates that fatigue life was in excess of the design curve for arc welding. When the fatigue joints efficiency is defined as fatigue limit of welds by that of BM, fatigue joints efficiencies of welds was 88%.

## REFERENCES

1. Eboo, M., Steen, W. M., and Clarke, J., "Arc Augmented Laser Welding," Imperial College London, pp. 257-265, 1979.
2. Beyer E., Dilthey U., Imhoff R., Maier C., Neuenhahn J., and Behler K., "New Aspects in Laser Welding with an Increased Efficiency," Proc. of SPIE Conference on Laser Materials Processing, pp.183-194, 1994.
3. Moon, J. H., Seo, P. K., and Kang, C. G., "A Study on Mechanical Properties of Laser-Welded Blank of a Boron Sheet Steel by Laser Ablation Variable of Al-Si Coating Layer," Int. J. Precis. Eng. Manuf., Vol. 14, No. 2, pp. 283-288, 2013.
4. Yang, R. T. and Chen, Z. W., "A Study on Fiber Laser Lap Welding of Thin Stainless Steel," Int. J. Precis. Eng. Manuf., Vol. 14, No. 2, pp. 207-214, 2013.
5. Dilthey, U. and Keller, H., "Prospects in Laser GMA Hybrid Welding of Steel," Proc. of International WLT Confernece on Lasers in Manufacturing, pp. 453-465, 2001.
6. Bagger, C. and Olsen, F. O., "Review of Laser Hybrid Welding," Journal of Laser Applications, Vol. 17, No. 1, pp. 2-14, 2005.
7. Zeyffarth, P. and Hoffmann, J., "Laser Technologies in Shipbuilding-Reality and Prospects," Paton Welding Journal C/C of Avtomaticheskaia Svarka, Vol. 2001, No. 12, pp. 9-15, 2001.
8. Herbert, S., "Laser-Hybrid Welding of Ships," Welding Journal, Vol. 83, No. 6, pp. 39-44, 2004.
9. Pan, L. K., Wang, C. C., Wei, S. L., and Sher, H. F., "Optimizing Multiple Quality Characteristics Via Taguchi Method-based Grey Analysis," Journal of Materials Processing Technology, Vol. 182,

No. 1, pp. 107-116, 2007.

10. Bang H. S., "Development of Laser-Arc Hybrid Welding Process and Evaluation of Mechanical Characteristics of Dissimilar Materials Welded Joints," Ph.D. Thesis, Div. Blob. Arch. and Urb. Desi., Osaka University, pp. 10-27, 2011.
11. Lloyd's Register of Shipping., "Guidelines for the Approval of CO2 Laser Welding," 1997.
12. ASM Handbook Committee, "ASM Handbook Vol. 8: Mechanical Testing," 1985.
13. ASM Hanbook Committee, "ASM Hanbook Vol. 19: Fatigue and Fracture," 1997.
14. Lloyd's Register of Shipping., "Rules for the Manufacture Testing and Certification of Materials," 2013.
15. Grevey, D., Sallamand, P., Cicala, E., and Ignat, S., "Gas Protection Optimization during Nd:YAG Laser Welding," Optics and Laser Technology, Vol. 37, No. 8, pp. 647-651, 2005.
16. Wang, H., Shi, Y., Gong, S., and Duan, A., "Effect of Assist Gas Flow on the Gas Shielding during Laser Deep Penetration Welding," Journal of Materials Processing Technology, Vol. 184, No. 1-3, pp. 379-385, 2007.
17. Campana, G., Fortunato, A., Ascari, A., Tani, G., and Tomesani, L., "The Influence of Arc Transfer Mode in Hybrid Laser-Mig Welding," Journal of Materials Processing Technology, Vol. 191, No. 1-3, pp. 111-113, 2007.
18. Fellman, A., Salminen, A., and Kujanpaa, V., "A Study of the Molten Filler Material Movements during CO2-laser-MAG Hybrid Welding," Proc. of WLT Conference on Lasers in Manufacturing, pp. 171-176, 2005.
19. Rates, M. E., Walz, C., and Sepold, G., "The Influence of Various Hybrid Welding Parameters on Bead Geometry," Welding Journal, Vol. 83, No. 5, pp. 147-153, 2004.
20. Fuhrmann, C., Petring, D., and Poprawe, R., "Recent Results on High Power CO2 and Nd: YAG Laser Arc Welding of Thick Steel Plates," Proc. of the 3rd International WLT-Conference on Lasers in Manufacturing, pp. 185-192, 2005.
21. Kutsuna, M. and Chen, L., "Interaction of both Plasmas in CO2 Laser-MAG Hybrid Welding of Carbon Steel," Proc. of SPIE 1st International Symposium on High-Power Laser Macroprocessing, Vol. 4831, pp. 341-346, 2003.
22. Ancona, A., Sibillano, T., Tricarico, L., Spina, R., Lugar, P. M., and et al., "Comparison of Two Different Nozzles for Laser Beam Welding of AA5083 Aluminium Alloy," Journal of Materials Processing Technology, Vol. 164-165, pp. 971-977, 2005.